ACS OMEGA

Article

http://pubs.acs.org/journal/acsodf

Tailoring the Diameters of Polyaniline Nanofibers for Sensor Application

Fuat Erden,[†,‡] Szu Cheng Lai,[†] Hong Chi,[§] FuKe Wang,*[,†] and Chaobin He*[,†,‡]

[†]Polymeric Materials Department, Institute of Materials Research and Engineering, Agency for Science, Technology and Research (A*STAR), 2 Fusionopolis Way, #08-03 Innovis, 138634 Singapore

[‡]Department of Materials Science and Engineering, National University of Singapore, 9 Engineering Drive 1, 117576 Singapore

[§]Shandong Provincial Key Laboratory of Fine Chemicals, School of Chemistry of Pharmaceutical Engineering, Qilu University of Technology, Jinan 250353, China

Supporting Information

ABSTRACT: Size control has been successfully achieved in inorganic materials, but it still remains a challenge in organic polymers due to their polydispersity. We here report a facial approach to tailor the diameter of polyaniline (PANI) nanofibers in a range of 200−30 nm via temperature-controlled polymerization from room temperature to −192 °C. It is shown that the formation of PANI nanofibers was directed by the self-assembly of an amphiphilic aniline−glutamic acid complex, which formed micelles with different sizes at various temperatures during polymerization. The size-dependent properties of the resulting PANI nanofibers, such as molecular weights, optical properties, crystallinity, and electron conductivity, have been discussed. Most importantly, we showed a more than 3 magnitude increase in the conductivities of doped PANI nanofibers with a decrease in the diameter from 150 to 30 nm. A homemade sensing device was constructed, and it is shown that PANI nanofibers with smaller diameters exhibit a much faster response than those of larger-sized fibers or bulk PANIs due to their large surface area and high intrinsic conductivities.

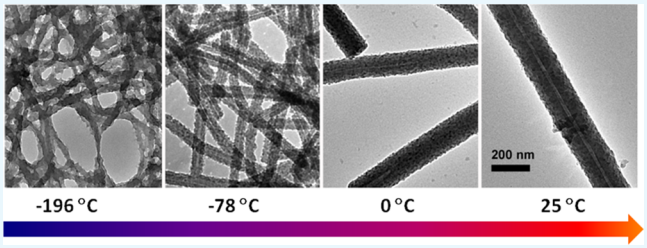

INTRODUCTION

Intrinsically conductive polymers and their nanostructured materials have attracted great interest because of their unique characteristics, such as tunable optical and electric properties and large surface areas, which have many potential applications, such as in batteries, electronic devices, electromagnetic interference, bio/chemical sensors, and chemical sensors.[1,2] Among various intrinsically conductive polymers, polyaniline (PANI) is one of the most studied and used polymers, owing to its unique nonredox doping/dedoping chemistry, high conductivity, and environmental stability.[3−7] Various types of nanostructures based on PANI, such as nanospheres, nanorods, nanosheets, and nanofibers, have been successfully prepared in the last decade,[8,9] and attempts have also been made by introducing porosity in the resulting nanostructures,[10,11] modifying the surface of the nanostructures with functional groups[12−14] or by coatings with metal nanoparticles.[15] Among these, the PANI nanofiber was a subject of numerous works, especially since the Kaner group developed the facile way to prepare nanofibers without the use of templates.[16,17] PANI nanofibers have shown greater sensitivity and faster time response compared to those of its conventional bulk counterpart due to a higher effective surface area and a shorter penetration depth for target molecules,[8] and the anisotropic geometry of nanofiber structures offers the possibility to use PANI nanofibers as building blocks for the fabrication of nonvolatile memories,[18] supercapacitors,[19,20] batteries,[21] catalysis support,[22] and chemical sensors.[23]

PANI nanofibers have been prepared by various techniques, such as soft and hard templating, interfacial polymerization, seeding polymerization, and so on.[6,16,17,24−29] However, in contrast to inorganic nanocrystals, the size control of PANI nanofibers is still a challenge, due mainly to the less monodisperse distribution of the size and shape of the PANI polymer chains.[30−33] Various techniques have been successfully developed to control the size of inorganic nanomaterials but have failed in tailoring the sizes of PANI nanofibers.

In this work, we report an effective way to control the sizes of the PANI nanofibers. The diameters of PANI nanofibers could be tailored from 200 to 30 nm by controlling the polymerization temperatures from room temperature to −192 °C. We showed the tunable optical and electronic properties of the resulting PANI nanofibers with different diameters, and a 6 × 10^3 increase in conductivity was observed for the PANI nanofibers with diameters changing from 200 to 30 nm. In addition, we demonstrated the size-dependent chemical response sensitivity of the PANI nanofibers.

Received: May 1, 2017
Accepted: May 23, 2017
Published: October 9, 2017

DOI: 10.1021/acsomega.7b00544
ACS Omega 2017, 2, 6506−6513

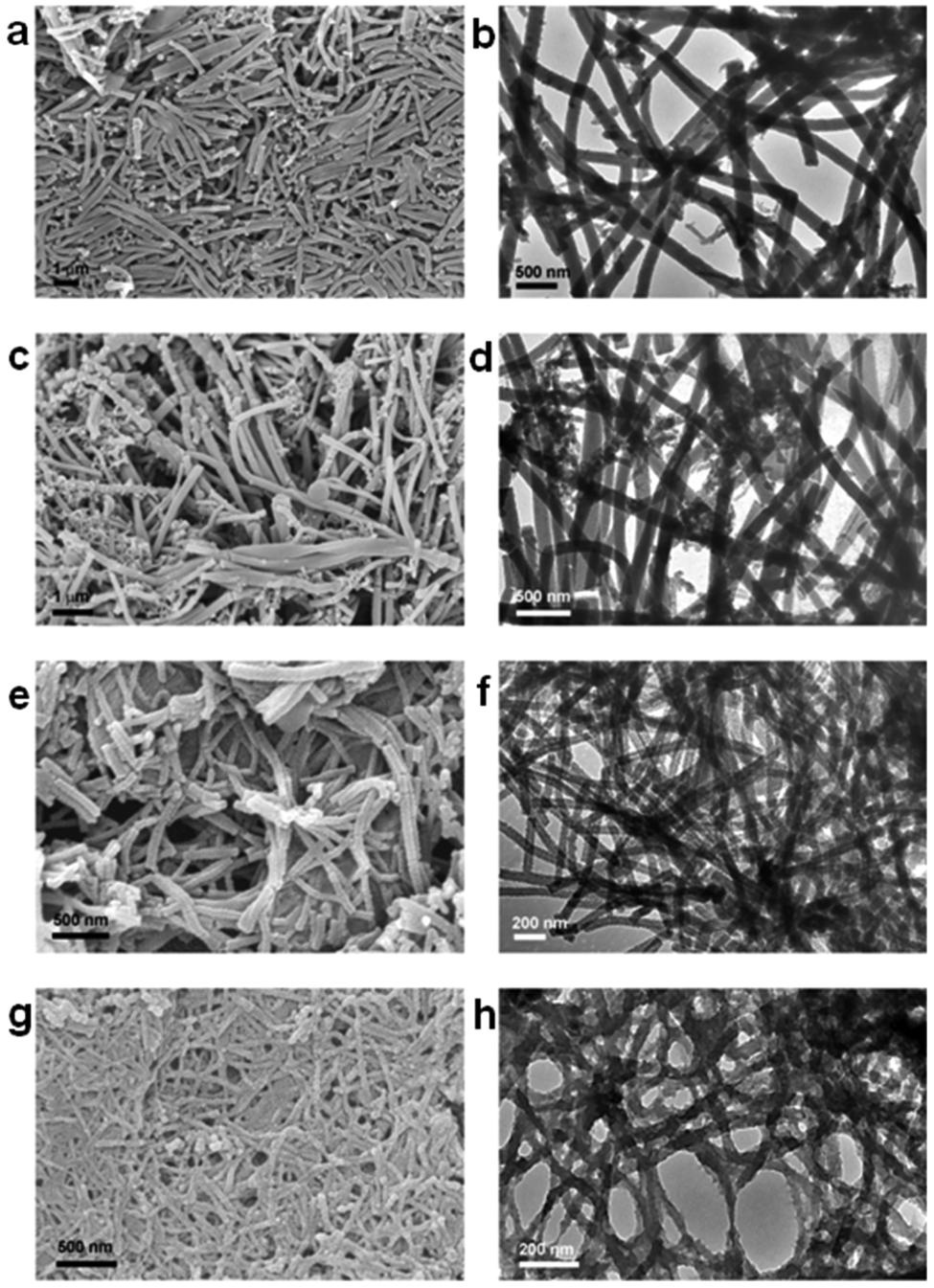

Figure 1. SEM (a, c, e, g) and transmission electron microscopy (TEM) (b, d, f, h) images of PANI nanofibers polymerized at different temperature: (a, b) 25 °C; (c, d) 0 °C; (e, f) −78 °C; (g, h) −192 °C.

RESULTS AND DISCUSSION

Tailoring the Diameters of PANI Nanofibers. Organic polymers cannot precisely and orderly crystallize as inorganic materials do, and most polymer nanoparticles form through self-assembly (aggregation) of the polymers.[34−36] Emulsion and precipitation techniques are the two main choices for the preparation of polymer nanoparticles, and with both these techniques it is difficult to control the size and shape of the polymers.[34−36] Therefore, we proposed that the size of the polymer nanoparticles could be tuned by controlling at the assembly step before polymerization, because the assembly of small molecules (monomers) is more precise than polymers. In the present work, we demonstrated that the diameters of PANI nanofibers could be tuned by controlling the assembly of monomers (anilines) before polymerization. As illustrated in our previous work,[25] aniline (monomer) and glutamic acid (Glu) first form a surfactant-like complex, which is self-assembled into nanorods (micelles) in solution. In addition, it is well known that the micelle sizes could be remarkably affected by the solution temperatures.[37,38] Thus, it is reasonable to assume that the sizes of micelles of the aniline−Glu complex could be tuned by changing the solution temperatures during assembly. To verify our hypothesis, anilines and Glu were first mixed in an aqueous solution, which was then put into a cooling bath at different temperatures during polymerization.

Figure 1 shows the electronic microscopy images of the four PANI nanofibers prepared at different polymerization temper-

DOI: 10.1021/acsomega.7b00544
ACS Omega 2017, 2, 6506−6513

atures from 25 to −192 °C. First, these products were found to consist predominantly of nanofibers alongside a small amount of granular PANI. As shown in the Supporting Information, in contrast to the traditional oxidative chemical polymerization route, which yields mainly granular PANI,[39] our method provides nearly 95% of PANI nanofibers, as can be seen in the low-magnitude scanning electron microscopy (SEM) image of a large area of the sample (Figure S1).

Both SEM and TEM images (Figure 1) show that the diameters of the obtained PANI nanofibers were significantly affected by the polymerization temperatures. The average diameters of PANI nanofibers prepared at room temperature (25 °C), in an ice-water bath (0 °C), in an acetone/dry ice bath (−78 °C), and in liquid nitrogen (−192 °C) are 200, 150, 60, and 30 nm, respectively. It is also interesting to note that the lower the polymerization temperature, the narrower the PANI nanofiber diameter distribution and larger the aspect ratio of the fibers.

The molecular structures of the pristine PANI nanofibers were characterized by Fourier transform infrared (FT-IR) spectroscopy, and the characteristic PANI bands were obtained (Figure 2). A strong and broad band at 3450 cm^{-1} is attributed

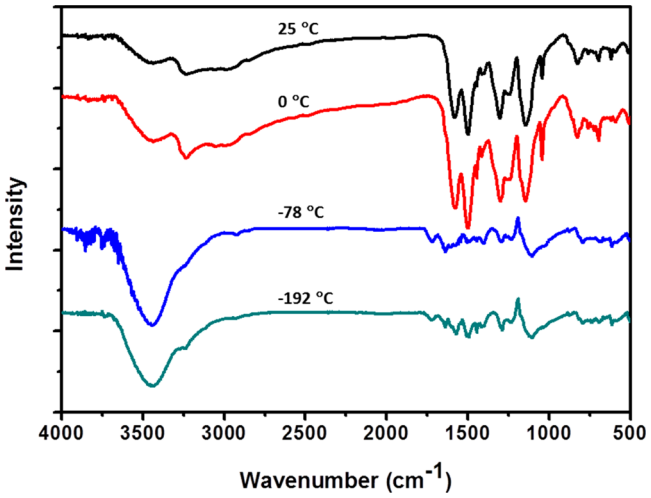

Figure 2. FT-IR spectra of PANI nanofibers prepared at different temperatures.

to the hydrogen-bonded N−H vibration.[40] Vibration peaks at around 1510 and 1580 cm^{-1} are ascribed to C═C stretching deformations of PANI benzenoid and quinoid rings, respectively. The peaks at 1300 and 1140 cm^{-1} correspond to C−N stretching and C−H bending vibration.[41] Strikingly, we found that PANI nanofibers polymerized at room temperature and the ice-water bath showed obvious characteristic peaks of Glu that appeared at about 3000 cm^{-1}, corresponding to the C−H stretching in the amino acid. However, there are no obvious Glu peaks in the FT-IR spectra of PANI nanofibers prepared at low temperatures of −78 and −192 °C. These results suggest that more Glu were buried in the PANI nanostructures that were synthesized at a higher temperature, whereas less Glu were left in the low-temperature polymerized PANI. This may be because Glu is easy to be removed from smaller-sized PANI nanofibers, which have a larger surface area. Or it may be due to the slow polymerization process at low temperatures that facilitates the diffusion of Glu out of the fibers, whereas at a high temperature, the rapid polymerization that starts on the surface would wrap Glu and hinder further diffusion of Glu out of the fiber.

To gain insight into the formation mechanism, powder X-ray diffraction (XRD) patterns of PANI nanofibers prepared at different temperatures were compared in Figure 3. A sharp peak

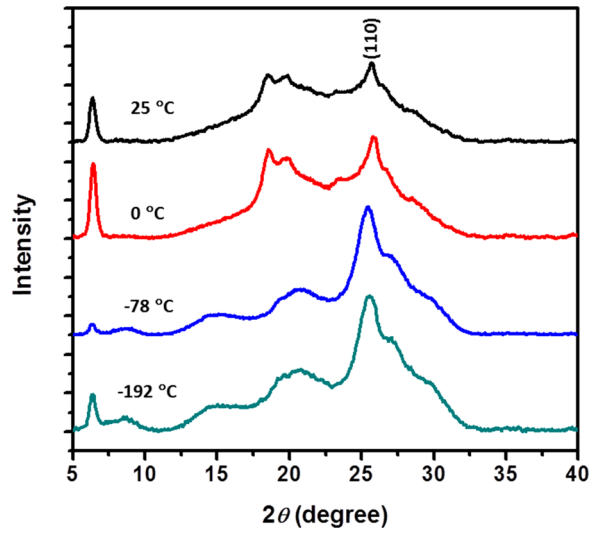

Figure 3. XRD patterns of PANI nanofibers prepared at different temperatures.

at 2θ = 25.6° was observed for all the PANI nanofibers synthesized at different temperatures, which was ascribed to the periodicity alignment of the PANI polymer chains.[42,43] The degree of crystallinity can be estimated from the area ratio of the crystalline peak to the amorphous peak. PANI nanofibers prepared at low temperatures (−78 and −192 °C) show a remarkable increase in the (110) peak intensity. The (110) reflection corresponds to the face-to-face interchain stacking distance between phenyl rings.[44] Therefore, the increase in the intensity of the (110) peak implies improved $\pi-\pi$ interchain stacking, suggesting that the structural ordering in the PANI chains increases with the decrease in the polymerization temperature. It is also interesting to note that strong XRD peaks were observed for PANI nanofibers synthesized at high temperatures (room temperature and 0 °C), centering at 2θ = 6.40, 18.5, and 19.8°. However, these peaks became weak for PANI nanofibers synthesized at lower temperatures of −78 and −192 °C. To better understand the XRD pattern, pure assembly of Glu with aniline without polymerization was studied for comparison. As described in our previous report, 25 equal molar ratios of aniline and Glu were mixed in deionized (DI) water to get a clear solution, which was frozen in an acetone/dry ice bath at −78 °C without adding the polymerization agent ammonium peroxydisulfate (APS). The resulting frozen mixture was dried using a freeze dryer. XRD pattern of the obtained white floccules showed sharp peaks at 2θ = 6.34, 17.4, 18.2, and 18.9°, suggesting that these peaks were mainly coming from the assembly of Glu and aniline (Figure S2). Therefore, we ascribed these peaks at 2θ = 6.40, 18.5, and 19.8° to the residues of crystallized Glu in the PANI polymer matrix. It is consistent with the FT-IR results that more Glu's were buried in the PANI nanofibers synthesized at higher temperatures.

The above information clearly suggests that the growth of PANI nanofibers was templated with Glu amino acids. It is

DOI: 10.1021/acsomega.7b00544
ACS Omega 2017, 2, 6506−6513

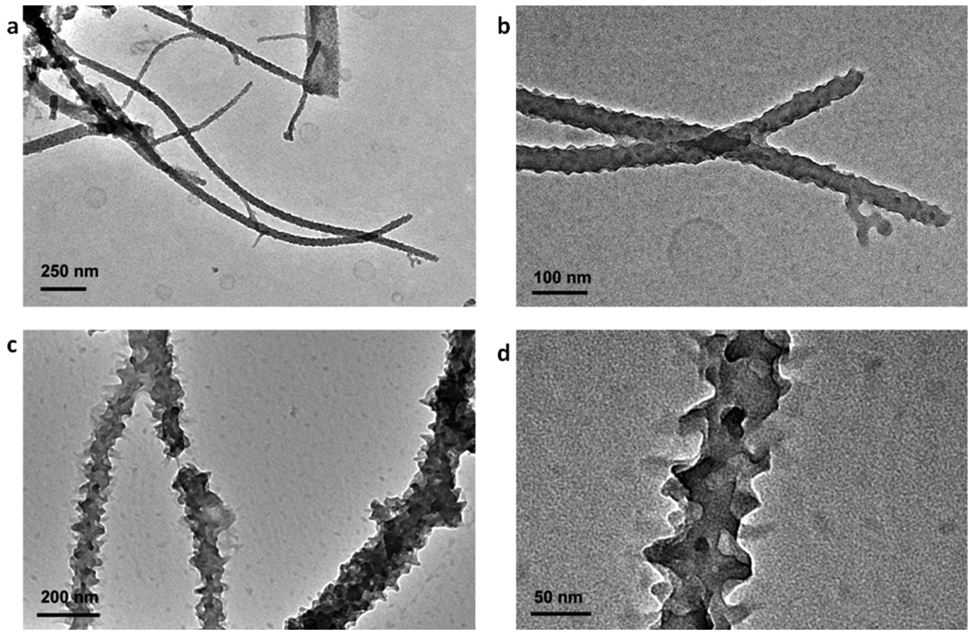

Figure 4. TEM images of PANI nanofibers at −192 °C with (a, b) and without (c, d) the presence of Glu.

generally believed that chemical oxidation polymerization of aniline with ammonium persulfate produces small oligomeric intermediates in the beginning of the reaction, which continue to grow through polymerization with aniline monomers or other oligomers. In our previous work, we had demonstrated that in DI water, the α-carboxylic acid in Glu can bind aniline through hydrogen bonding, forming the amphiphilic aniline−Glu complex. The formed complex would self-assemble in water and form the nanorod structures as observed in the SEM images.[25] The subsequent PANI nanofiber growth was directed by these nanorods. The sizes of the nanorods formed from the amphiphilic aniline−Glu complex may change at different polymerization temperatures and thus tune the diameters of the resulting PANI nanofibers.[37,38]

However, at an extremely low temperature (−192 °C), due to a fast cooling and quick freezing of water, ice was formed during the assembly of the amphiphilic aniline−Glu complex. Thus, the formation of PANI nanofibers was directed not only by the assembly of the aniline−Glu complex but also by the ice crystal template.[45,46] To confirm the role of ice-templating in the formation of PANI nanofibers at low temperatures, the oxidative polymerization of aniline by APS without Glu was carried out in liquid nitrogen. As shown in Figure 4, PANI nanofibers with a fish-bone surface were obtained with a diameter of about 50 nm. On comparing the PANI nanofibers synthesized at −192 °C with and without the Glu template, it can be observed that the obtained nanofibers in the presence of Glu templates exhibit a relatively smooth surface and smaller diameters, suggesting that the assembly of the aniline−Glu complex plays a major role in directing the formation of PANI nanofibers at −192 °C.

Optical and Electronic Properties of PANI Nanofibers. A UV−visible spectroscopy analysis was carried out to further investigate the oxidation levels of PANI nanofibers. Similar to the PANI spectra report, a dark green emeraldine form was obtained with a distinctive polaron band at wavelengths beyond 800 nm when PANI nanofibers were doped with a 1 M HCl solution (Figure 5a).[18] When it was dedoped with a 1 M ammonium solution, a purple-colored solution led to a nonconducting form, with characteristic absorption at around 600 nm (Figure 5b). A strong peak was observed at 350 nm for both doped and undoped samples, which was assigned to the

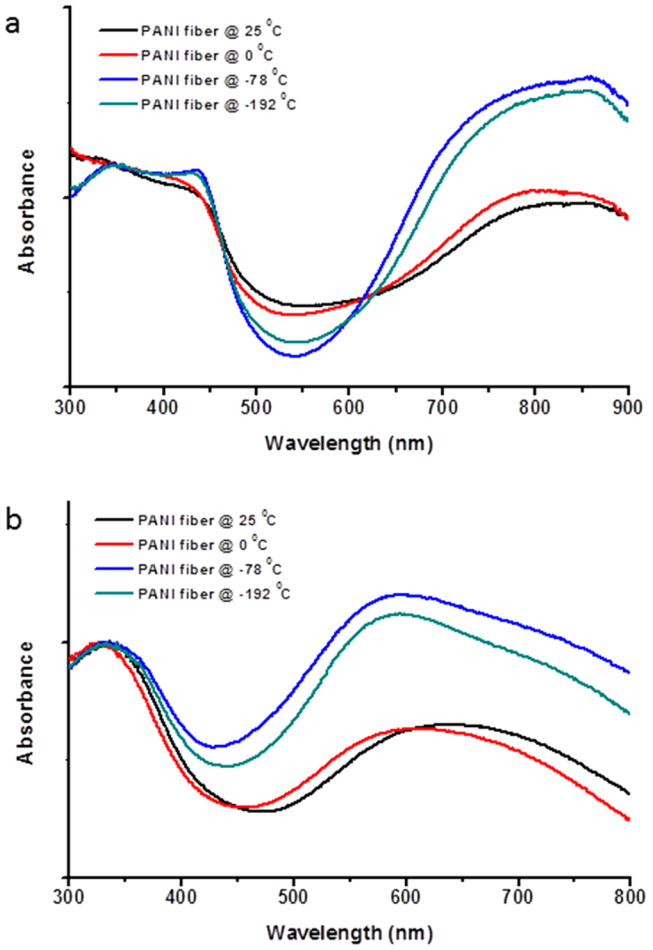

Figure 5. UV−vis spectroscopy analysis of doped (a) and dedoped (b) PANI nanofibers polymerized at different temperatures.

DOI: 10.1021/acsomega.7b00544
ACS Omega 2017, 2, 6506−6513

$\pi-\pi^*$ transition (within the benzenoid segment) in pure PANI samples.[47,48] The average oxidation level of the PANI nanofibers can be measurable by comparison of the ratio of the absorbance of the polaronic band to that of the $\pi-\pi^*$ transition.[44] Judged from the peak ratios of $A880/A350$ nm, it can be seen clearly that PANI nanofibers with smaller diameters appear to be in the higher oxidation level.

The conductivities of the synthesized PANIs were measured by using the Keithley four-point probe method, and the results are listed in Table 1. Conductivity results showed that the as-synthesized PANI nanofibers have a much higher conductivity than the reported neutral PANIs. This is because the as-synthesized PANIs were partially doped with Glu. The obtained PANI was then dedoped with ammonium oxide (0.1 M) overnight and then redoped with camphorsulfonic acid (CSA), and the conductivity was generally increased about 1 or 2 magnitudes. Most importantly, we found that the conductivities of both the pristine and redoped PANI nanofibers showed a remarkable increase with the decrease in the diameters of the PANI nanofibers. For CSA-doped PANI nanofibers, the conductivity of PANI synthesized at −192 °C is more than 3 magnitudes higher than that prepared at room temperature.

Table 1. Electrical Conductivity Results of the As-Synthesized and Redoped PANI Nanofibers

polymerization temperature (°C)	conductivity of as-synthesized PANI nanofibers (S/cm)	conductivity of the re-doped PANI nanofibers (S/cm)
25	2.5×10^{-5}	1.37×10^{-4}
0	4.0×10^{-4}	9.8×10^{-4}
−78	2.45×10^{-2}	0.16
−192	1.12×10^{-2}	0.92

The high conductivities of the PANI nanofibers synthesized at lower temperatures than those prepared at higher temperatures may be due to the different fiber sizes, crystallinity, and molecular weight of the polymer. Generally, the smaller diameter induces a larger contact surface, which leads to a larger contacting area in the pressed PANI nanofiber pellets for the conductivity measurement. In addition, we noted that PANI nanofibers prepared at low temperatures showed increased crystallinity and intensity of (110) peak, suggesting improved $\pi-\pi$ interchain stacking in the smaller-diameter PANI nanofibers. The better structural ordering leads to enhanced charge-carrier transport through elongation of the effective conjugation length.

Furthermore, it has been reported that the conductivity of PANI was also affected by the molecular weights of the polymer. That is, the longer the conjugated polymer chain, the longer the electron delocalization.[3,49] We measured the intrinsic viscosity of the synthesized PANIs to estimate the relative molecular weight of the obtained PANI nanofibers. As shown in the specific viscosity measurement results (Figure S3 and Table S1), the intrinsic viscosity (dL/g) of PANIs (dissolved in *N*-methyl-2-pyrrolidone (NMP)) are 13.22, 21.28, 36, and 54.32 for the fibers synthesized at 25, 0, −78, and −192 °C, respectively, suggesting an increasing molecular weight of the prepared PANI nanofibers with decreasing polymerization temperature.

Size-Dependent Chemical Sensitivity of PANI Nanofibers. The formed PANI nanofibers showed significant enhancement of chemical sensitivity compared to that of the bulky PANI prepared by a traditional oxidative polymerization method. To demonstrate the gas sensitivity of the obtained PANI nanofibers, a homemade gas sensor was constructed using an SPI silver paste with the help of a 3 mm wide tape as a mask (Figure S4). After annealing the silver paste at 120 °C for 1 h, one drop of the dedoped PANI aqueous solution was solution-cast on the gas sensor between the two electrodes and dried in atmosphere overnight. The gas sensor was then connected to a digital multimeter, and the device was sealed in a chamber filled with 1 M HCl solution with stirring. For comparison, bulky PANI was also prepared by traditional APS oxidative polymerization of aniline in an aqueous solution and then dedoped with a 1 M ammonium solution overnight. The dedoped PANIs were not conductive with a resistance of few GΩ, but their resistance rapidly changed to a few MΩ or tens of KΩ in minutes. Figure 6 shows the typical response data for dedoped PANI exposed to 100 ppm of HCl vapor. The resistances of the dedoped PANI nanofibers show faster and larger response to acid vapor than the bulky PANI. Resistances of dedoped PANI nanofibers changed by 3−5 orders of magnitude on exposure to the HCl vapor, and the smaller the diameter of nanofibers, the faster the response time.

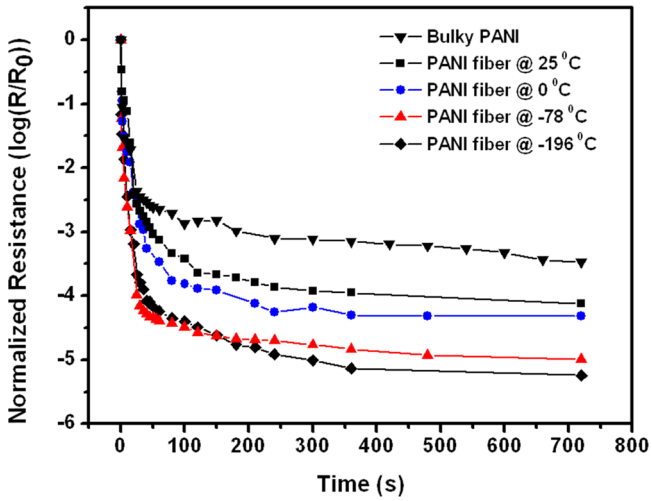

Figure 6. Normalized resistance measured vs time upon exposure of dedoped PANI to 100 ppm of HCl with bulky PANI and different sizes of PANI nanofibers.

The size-dependent sensor response was attributed to the following factors. First, the sensor response is dependent on the diffusion of the acid vapor through the PANI film on the gas sensor, which is affected by the surface area and the porosity of the film. The smaller the diameter of the PANI nanofibers, the faster is the response to the acid vapor because the surface area is inversely related to the nanofiber diameters. Moreover, TEM images of the PANI nanofiber showed that the nanofiber prepared at a lower temperature has a more rough surface as compared to that prepared at a temperature above 0 °C. Second, the greatly enhanced sensor capability of the smaller-sized PANI nanofibers that were prepared at a low temperature may also be related to their higher conductivities, as we have discussed above.

CONCLUSIONS

In summary, a facile synthetic approach to tune the diameters of PANI nanofibers and their size-dependent sensing application were demonstrated. Our results showed that the

DOI: 10.1021/acsomega.7b00544
ACS Omega 2017, 2, 6506−6513

growth of PANI nanofibers was directed by the assembly of the amphiphilic aniline−Glu complex, and the sizes of micelles of the complex could be controlled by the polymerization temperatures. In addition, the formation of ice at extremely low temperatures also plays a part in controlling the fiber diameter. The structural, optical, and electronic properties of PANI nanofibers synthesized at different temperatures were discussed. We showed a more than 3 magnitude increase of the conductivities of PANI nanofibers with diameters changing from 200 to 30 nm. The application of the size-controlled PANI nanofibers in a gas sensor was also demonstrated. This work provides a way for constructing more sensitive PANI-based sensors, together with the potential applications in the fields of catalysis, supercapacitors, and memories.

EXPERIMENTAL SECTION

Materials. Aniline (≥99%) was purchased from Aldrich and vacuum-distilled before use. APS, Glu (99%), NMP, and CSA were purchased from Aldrich and used as received without further purification. DI water (18.2 MΩ) was used throughout the experiment, and all glassware was cleaned using concentrated nitric acid and subsequently rinsed with a copious amount of DI water.

Preparation of PANI Nanofibers. PANI nanofibers were synthesized by a chemical oxidation polymerization method in the presence of amino acid templates, as reported previously.[25] Typically, 1 mmol (0.147 g) L-Glu was added into 10 mL of DI water and quickly degassed with Argon gas for 2 min. The reactor was put into an ultrasonication bath for 10 min with an ice-water bath. Then, freshly distilled aniline (1 mmol, 92 μL) was added to the mixture in one portion, and the reactor was put in the ultrasonication bath again until both aniline and L-Glu were dissolved to give a clear solution.

In another reactor, 1 mmol of APS (0.228 g) was dissolved in 2 mL of water with the help of ultrasonication. The APS solution was then rapidly added into the clear mixture of aniline and L-Glu with gentle shaking for about 10 s without color change. The reaction mixture was then put into a water bath at 25 °C and kept at this temperature for 8 h. The reaction mixture was left without disturbing overnight. The obtained PANI fibers were separated by centrifugation of the reaction mixture at 8000 rpm for 15 min, and the centrifuge pellets were redispersed in DI water. The centrifugation and washing with DI water was repeated for several cycles until the supernatant became light green.

The PANI nanofibers synthesized at different temperatures were prepared by the same method, except the mixed APS and aniline were put into different cooling baths: ice-water bath (0 °C), acetone/dry ice bath (−78 °C), and liquid nitrogen (−192 °C). For the PANI nanofibers synthesized at low temperatures (−78 and −192 °C), a further 2 h reaction at room temperature is required to complete the polymerization. The yields of the obtained PANI nanofibers were in the range of 35−45%. The outer diameter of the obtained PANI nanofibers that were prepared at room temperature (25 °C), in an ice-water bath (0 °C), in an acetone/dry ice bath (−78 °C), and in liquid nitrogen (−192 °C) were found to be 200, 150, 60, and 30 nm, respectively. The corresponding aspect ratios were found to be 12, 18, 22, and 33.

Characterization. SEM images of the samples were obtained by using a JEOL field-emission scanning electron microscope (FESEM) JSM6700F FESEM at 5 kV acceleration voltages. TEM micrographs were obtained using a JEOL 2100TEM operating at an accelerating voltage of 200 kV. A drop of the sample dispersed in water was cast onto a 200-mesh carbon-coated copper grid. The samples were dried at room temperature before measurement.

UV−vis spectra were recorded on a Shimadzu 3600 UV−vis near-infrared (UV−vis−NIR) Spectrophotometer. The XRD pattern measurement was done on a Bruker D8 General Area Detector Diffraction System with Cu Kα radiation. Samples for XRD analysis was prepared by drop-casting of the sample solution onto a silicon wafer substrate and dried at room temperature. The cyclic voltammograms of PANI nanofibers were carried out on an Auto lab potentiostat. PANI fibers were deposited on glass carbon and used as a working electrode. Pt and Ag/AgCl (3 M KCl) electrodes were used as counter and reference electrodes, respectively.

The molecular weight of PANI was measured by a Cannon-Ubbelohde dilution viscometer at room temperature. The efflux time for NMP was recorded at first as a reference. Synthesized PANI (50 mg) was dissolved in 10 mL of NMP containing LiCl (0.2 wt %), and the efflux time was recorded. Then, the PANI solution was diluted by adding 5 mL of NMP−LiCl (0.2 wt %), and the efflux time was measured again. This step was repeated until final solution contained 25 mL of the NMP−LiCl solvent. The relative molecular weight of PANI was compared by its relative calculated intrinsic viscosity.

The Keithley four-point probe system at room temperature was used for the electrical conductivity test. In a typical measurement, a constant current was passed through the two outer probes, and the corresponding potential drop across the middle two probes was measured. The current was systematically increased four times, and corresponding potential drop values were recorded. All measurements were repeated at four different contact points on the surface, and the average values were calculated. Then, the current versus voltage graph was plotted, and the slope of the graph was used for the calculation of resistivity and hence conductivity.

ASSOCIATED CONTENT

Supporting Information

The Supporting Information is available free of charge on the ACS Publications website at DOI: 10.1021/acsomega.7b00544.

Low-magnitude SEM image of PANI nanofibers, XRD patterns of assemblies of the amphiphilic aniline−Glu complex; specific viscosity change as a function of polymer concentrations of PANI nanofibers; table of intrinsic viscosity results of PANI nanofibers synthesized at different temperatures, and the scheme of the homemade gas sensor and testing (PDF)

AUTHOR INFORMATION

Corresponding Authors

*E-mail: wangf@imre.a-star.edu.sg (F.W.).
*E-mail: cb-he@imre.a-star.edu.sg (C.H.).

ORCID

FuKe Wang: 0000-0002-6980-5857
Chaobin He: 0000-0001-8200-8337

Author Contributions

The manuscript was prepared through contributions of all authors.

Notes

The authors declare no competing financial interest.

DOI: 10.1021/acsomega.7b00544
ACS Omega 2017, 2, 6506−6513

■ ACKNOWLEDGMENTS

We acknowledge financial support of this work from the Science and Engineering Research Council (Grant 1527200019) of Agency for Science, Technology and Research of Singapore. F.E. also acknowledges scholarship support from the Singapore International Graduate Award (SINGA).

■ REFERENCES

(1) Hatchett, D. W.; Josowicz, M. Composites of Intrinsically Conducting Polymers as Sensing Nanomaterials. *Chem. Rev.* **2008**, *108*, 746−769.
(2) Nguyen, D. N.; Yoon, H. Recent Advances in Nanostructured Conducting Polymers: from Synthesis to Practical Applications. *Polymers* **2016**, *8*, 118.
(3) MacDiarmid, A. G. Polyaniline and polypyrrole: where are we headed? *Synth. Met.* **1997**, *84*, 27−34.
(4) MacDiarmid, A. G. "Synthetic Metals": A Novel Role for Organic Polymers (Nobel Lecture). *Angew. Chem., Int. Ed.* **2001**, *40*, 2581−2590.
(5) Hu, L. B.; Gruner, G.; Li, D.; Kaner, R. B.; Cech, J. Patternable Transparent Carbon Nanotube Films for Electrochromic Devices. *J. Appl. Phys.* **2007**, *101*, No. 016102.
(6) Joseph, N.; Varghese, J.; Sebastian, M. T. Self-Assembled Polyaniline Nanofibers with Enhanced Electromagnetic Shielding Properties. *RSC Adv.* **2015**, *5*, 20459−20466.
(7) Joseph, N.; Varghese, J.; Sebastian, M. T. A Facile Formulation and Excellent Electromagnetic Absorption of Room Temperature Curable Polyaniline Nanofiber Based Inks. *J. Mater. Chem. C* **2016**, *4*, 999−1008.
(8) Li, D.; Huang, J.; Kaner, R. B. Polyaniline Nanofibers: A Unique Polymer Nanostructure for Versatile Applications. *Acc. Chem. Res.* **2009**, *42*, 135−145.
(9) Tran, H. D.; D'Arcy, J. M.; Wang, Y.; Beltramo, P. J.; Strong, V. A.; Kaner, R. B. The Oxidation of Aniline to Produce "Polyaniline": A Process Yielding Many Different Nanoscale Structures. *J. Mater. Chem.* **2011**, *21*, 3534−3550.
(10) Paik, P.; Manda, R.; Amgoth, C.; Kumar, K. S. Polyaniline Nanotubes with Rectangular-Hollow-Core and Its Self-Assembled Surface Decoration: High Conductivity and Dielectric Properties. *RSC Adv.* **2014**, *4*, 12342−12352.
(11) Paik, P.; Mastai, Y.; Gedanken, A. Chiral-mesoporous-polypyrrole Nanoparticles: Its Chiral Recognition Abilities and Use in Enantioselective Separation. *J. Mater. Chem.* **2010**, *20*, 4085−4093.
(12) Wulff, G. Molecular Imprinting in Cross-Linked Materials with the Aid of Molecular Templates - A Way towards Artificial Antibodies. *Angew. Chem., Int. Ed.* **1995**, *34*, 1812−1832.
(13) Wang, B.; Chi, C.; Shan, W.; Zhang, Y. H.; Ren, N.; Yang, W. L.; Tang, Y. Chiral Mesostructured Silica Nanofibers of MCM-41. *Angew. Chem., Int. Ed.* **2006**, *45*, 2088−2090.
(14) Che, S.; Liu, Z.; Ohsuna, T.; Sakamoto, K.; Terasaki, O.; Tatsumi, T. Synthesis and Characterization of Chiral Mesoporous Silica. *Nature* **2004**, *429*, 281−284.
(15) Chowdhury, D. Ni-Coated Polyaniline Nanowire as Chemical Sensing Material for Cigarette Smoke. *J. Phys. Chem. C* **2011**, *115*, 13554−13559.
(16) Huang, J.; Kaner, R. B. A General Chemical Route to Polyaniline Nanofibers. *J. Am. Chem. Soc.* **2004**, *126*, 851−855.
(17) Tran, H. D.; Kaner, R. B. A General Synthetic Route to Nanofibers of Polyaniline Derivatives. *Chem. Commun.* **2006**, 3915−3917.
(18) Tseng, R. J.; Huang, J.; Ouyang, J.; Kaner, R. B.; Yang, Y. Polyaniline Nanofiber/Gold Nanoparticle Non-volatile Memory. *Nano Lett.* **2005**, *5*, 1077−1080.
(19) Zhang, K.; Zhang, L. L.; Zhao, X. S.; Wu, J. Graphene/Polyaniline Nanofiber Composites as Supercapacitor Electrodes. *Chem. Mater.* **2010**, *22*, 1392−1401.
(20) Hyder, M. N.; Lee, S. W.; Cebeci, F. C.; Schmidt, D. J.; Shao-Horn, Y.; Hammond, P. T. Layer-by-Layer Assembled Polyaniline Nanofiber/Multiwall Carbon Nanotube Thin Film Electrodes for High-Power and High-Energy Storage Applications. *ACS Nano* **2011**, *5*, 8552−8561.
(21) Ghenaatian, H. R.; Mousavi, M. F.; Rahmanifar, M. S. High Performance Battery-Supercapacitor Hybrid Energy Storage System Based on Self-Doped Polyaniline Nanofibers. *Synth. Met.* **2011**, *161*, 2017−2023.
(22) Chang, G.; Luo, Y.; Lu, W.; Qin, X.; Asiri, A. M.; Al-Youbi, A. O.; Sun, X. Ag Nanoparticles Decorated Polyaniline Nanofibers: Synthesis, Characterization, and Applications toward Catalytic Reduction of 4-nitrophenol and Electrochemical Detection of H_2O_2 and Glucose. *Catal. Sci. Technol.* **2012**, *2*, 800−806.
(23) Liao, Y.; Zhang, C.; Zhang, Y.; Strong, V.; Tang, J.; Li, X.-G.; Kalantar-Zadeh, K.; Hoek, E. M. V.; Wang, K. L.; Kaner, R. B. Carbon Nanotube/Polyaniline Composite Nanofibers: Facile Synthesis and Chemosensors. *Nano Lett.* **2011**, *11*, 954−959.
(24) Tang, Q.; Wu, J.; Sun, X.; Li, Q.; Lin, J.; Huang, M. Templateless Self-assembly of Highly Oriented Polyaniline Arrays. *Chem. Commun.* **2009**, 2166−2167.
(25) Wang, F. K.; Wang, Z.; Tana, M. B. H.; He, C. Uniform Polyaniline Nanotubes Formation via Frozen Polymerization and Application for Oxygen Reduction Reactions. *Macromol. Chem. Phys.* **2015**, *216*, 977−984.
(26) Zhang, L.; Long, Y.; Chen, Z.; Wan, M. The Effect of Hydrogen Bonding on Self-Assembled Polyaniline Nanostructures. *Adv. Funct. Mater.* **2004**, *14*, 693−698.
(27) Wan, M. A Template-Free Method Towards Conducting Polymer Nanostructures. *Adv. Mater.* **2008**, *20*, 2926−2932.
(28) Rana, U.; Chakrabartib, L.; Malik, S. Benzene tetracarboxylic acid doped polyaniline nanostructures: morphological, spectroscopic and electrical characterization. *J. Mater. Chem.* **2012**, *22*, 15665−15671.
(29) Rana, U.; Mondal, S.; Sannigrahi, J.; Sukul, P. K.; Amin, M. A.; Majumdar, S.; Malik, S. Aromatic bi-, tri- and tetracarboxylic acid doped polyaniline nanotubes: effect on morphologies and electrical transport properties. *J. Mater. Chem. C* **2014**, *2*, 3382−3389.
(30) Yan, Z.; Xu, H.; Guang, S. A Convenient Organic-inorganic Hybrid Approach toward Highly Stable Squaraine Dyes with Reduced H-Aggregation. *Adv. Funct. Mater.* **2012**, *22*, 345−352.
(31) Tao, Y.; Li, J.; Xie, A.; Li, S.; Chen, P.; Ni, L.; Shen, Y. Supramolecular Self-Assembly of Three-Dimensional Polyaniline and Polypyrrole Crystals. *Chem. Commun.* **2014**, *50*, 12757−12760.
(32) Zhang, X.; Manohar, S. K. Polyaniline Nanofibers: Chemical Synthesis Using Surfactants. *Chem. Commun.* **2004**, *40*, 2360−2361.
(33) Li, G.; Jiang, L.; Peng, H. One-dimensional Polyaniline Nanostructures with Controllable Surfaces and Diameters Using Vanadic Acid as the Oxidant. *Macromolecules* **2007**, *40*, 7890−7894.
(34) Yu, H.; Kim, D. Y.; Lee, K. J.; Oh, J. H. Fabrication of One Dimensional Organic Nanomaterials and their Optoelectronic Applicatios. *J. Nanosci. Nanotechnol.* **2014**, *14*, 1282−1302.
(35) Pecher, J.; Mecking, S. Nanoparticles of Conjugated Polymers. *Chem. Rev.* **2010**, *110*, 6260−6279.
(36) Wang, F. K.; Han, M. Y.; Mya, K. Y.; Wang, Y.; Lai, Y.-H. Aggregation-driven Growth of Size-tunable Organic Nano Particles Using Electronically Altered Conjugated Polymers. *J. Am. Chem. Soc.* **2005**, *127*, 10350−10355.
(37) Balmbra, R. R.; Clunie, J. S.; Corkill, J. M.; Goodman, J. F. Effect of Temperature on Micelle Size of a Homogeneous Non-ionic Detergent. *Trans. Faraday Soc.* **1962**, *58*, 1661−1667.
(38) Nicoli, D. F.; Ciccolello, R.; Briggs, J.; Dawson, D. R.; Offen, H. W.; Romsted, L.; Bunton, C. A. Micellar Size as a Function of Pressure, Temperature, and Salt Concentration for a Series of Cationic Surfactants. In *NATO Advanced Study Institutes Series*; Springer, 1981; Vol. *73*, pp 363−380.
(39) Huang, W. S.; Humphrey, B. D.; MacDiarmid, A. G. Polyaniline, a Novel Conducting Polymer. *J. Chem. Soc., Faraday Trans. 1* **1986**, *82*, 2385−2400.

DOI: 10.1021/acsomega.7b00544
ACS Omega 2017, 2, 6506−6513

(40) Kilmartin, A.; Wright, G. A. Photoelectrochemistry and Spectroscopy of Substituted Polyanilines. *Synth. Met.* **1999**, *104*, 145−156.
(41) Liu, Z.; Zhu, Y.; Wang, L.; Ding, C.; Wang, N.; Wan, M.; Jiang, L. Polyaniline microtubes with a Hexagonal Cross-Section and pH-Sensitive Fluorescence Properties. *Macromol. Rapid Commun.* **2011**, *32*, 512−517.
(42) Pouget, J. P.; Jozefowicz, M. E.; Epstein, A. J.; Tang, X.; MacDiarmid, A. G. X-ray Structure of Polyaniline. *Macromolecules* **1991**, *24*, 779−789.
(43) Yang, Y.; Wan, M. Chiral Nanotubes of Polyaniline Synthesized by a Template-Free Method. *J. Mater. Chem.* **2002**, *12*, 897−901.
(44) Park, H.-W.; Kim, T.; Huh, J.; Kang, M.; Lee, J. E.; Yoon, H. Anisotropic Growth Control of Polyaniline Nanostructures and Their Morphology-Dependent Electrochemical Characteristics. *ACS Nano* **2012**, *6*, 7624−7633.
(45) Ihara, H.; Yoshitake, M.; Takafuji, M.; Yamada, T.; Sagawa, T.; Hirayama, C.; Hachisako, H. Detection of Highly Oriented Aggregation of L-Glutamic Acid Derived Lipids in Dilute Organic Solution. *Liq. Cryst.* **1999**, *26*, 1021−1027.
(46) Zhang, L.; Peng, H.; Zujovic, Z. D.; Kilmartin, P. A.; Travas-Sejdic, J. Characterization of Polyaniline Nanotubes Formed in the Presence of Amino Acids. *Macromol. Chem. Phys.* **2007**, *208*, 1210−1217.
(47) Liu, W.; Kumar, J.; Tripathy, S.; Senecal, K. J.; Samuelson, L. Enzymatically Synthesized Conducting Polyaniline. *J. Am. Chem. Soc.* **1999**, *121*, 71−78.
(48) Feng, X.; Yang, G.; Xu, Q.; Hou, W.; Zhu, J.-J. Self-Assembly of Polyaniline/Au Composites from Nanotubes to Nanofibers. *Macromol. Rapid Commun.* **2006**, *27*, 31−36.
(49) Bhadra, S.; Khastgir, D.; Singha, N. K.; Lee, J. H. Progress in Preparation, Processing and Applications of Polyaniline. *Prog. Polym. Sci.* **2009**, *34*, 783−810.

DOI: 10.1021/acsomega.7b00544
ACS Omega 2017, 2, 6506−6513